Chinese Chemical Letters 37 (2026) 111671

Contents lists available at ScienceDirect

Chinese Chemical Letters

journal homepage: www.elsevier.com/locate/cclet

Advances in preparation and modification strategies of CeO_2 nanozymes and potential clinical applications

Zhixuan Li, Xinying Wang, Han Wu, Qingxiang Guan*

School of Pharmaceutical Sciences, Jilin University, Changchun 130021, China

ARTICLE INFO

Article history:
Received 9 June 2025
Revised 30 July 2025
Accepted 2 August 2025
Available online 7 August 2025

Keywords:
Cerium oxide
Nanozymes
Green preparation methods
Modification strategies
Clinical applications

ABSTRACT

Cerium oxide nanozymes (CeO_2 NZs) exhibit enzyme mimetic activities and great promise for biomedical applications by mediating the dynamic cycling between Ce^{3+} and Ce^{4+}. However, traditional preparation methods are often expensive and detrimental to the environment. Meanwhile, the problems of easy agglomeration, poor targeting and weak biocompatibility need to be solved. The available literatures have mainly reviewed CeO_2 NZs in terms of its material properties, mechanisms and potential clinical applications. The literatures on the limitations of CeO_2 NZs and the corresponding improvement methods are fragmented. Consequently, the limitations of CeO_2 NZs and the strategies involving green preparation technology and modification mainly summarized, while the biosafety of the modification strategies are compared. Meanwhile, representative studies of potential clinical applications of CeO_2 NZs over the past three years are outlined, along with a summary of their clinical translational prospects and challenges. Finally, the challenges of CeO_2 NZs promotion technology are discussed.

© 2026 Published by Elsevier B.V. on behalf of Chinese Chemical Society and Institute of Materia Medica, Chinese Academy of Medical Sciences.

1. Introduction

Natural enzymes have the advantages of high substrate affinity, specificity and superior biocompatibility compared with chemical drugs. However, the disadvantages involving the susceptibility to inactivation, shorter half-life and higher purity requirements for application hinder their further development in the clinical applications [1–3].

In 2004, gold nanoparticles (NPs) are firstly found to can catalyze the phosphodiester bond cleavage reaction and name them as nanozymes (NZs) [4]. In 2007, it is reported Fe_3O_4 NPs endowing peroxidase (POD) mimetic activity can break the boundaries between inorganic materials and biological activities [5]. NZs have the advantage of mimicking a wide range of enzyme activities, higher stability as well as the ease of surface modification and modulation of catalytic activity facilitating complex biochemical reactions in comparison to natural enzymes [6–8]. CeO_2 is one of the most common nanozymes. CeO_2 NZs have a reversible cycling between Ce^{3+} (reduced state) and Ce^{4+} (oxidized state), thereby generating oxygen vacancies in the lattice structure, which presents excellent oxygen storage and releases capacity, redox activity and enzyme-like catalytic activities [9–11]. The multiple enzyme-like activities evoke a wide range of research perspectives in diagnosis and therapy in the biomedical field [12,13]. It is worth noting some limitations of CeO_2 NZs in aspect of the preparation and application studies hamper its large-scale production and potential applications. Interestingly, the green preparation methods developed in recent years are environmentally beneficial and economical. Besides, the synthesized NPs are more stable [14,15]. Meanwhile, surface modification and cell membrane biomimetic modification strategies are utilized to prevent the agglomeration of CeO_2 NZs and elevate the biocompatibility as well as targeting [16–18]. In addition, doping modification strategies can further accelerate the catalytic performance and enzyme mimetic activities of CeO_2 NZs *via* promoting changes in surface physicochemical properties [19,20].

Currently, the reviews on CeO_2 NZs mainly cover their action mechanism, promising biomedical applications. However, the literatures on the limitations of CeO_2 NZs and the corresponding improvement methods are fragmented and systematic reviews are lack. Herein, the shortcomings of its traditional preparation methods of CeO_2 NZs are introduced. The novel progress of its green preparation methods is summarized and discussed. Meanwhile, surface modification, cell membrane biomimetic and doping modification strategies are emphatically analyzed and discussed, and the three approaches are compared in terms of biosafety. Additionally, representative potential biological applications of CeO_2 NZs in recent years are outlined, along with a summary of their clinical translational prospects and challenges (Fig. 1).

* Corresponding author.
E-mail address: guanqx@jlu.edu.cn (Q. Guan).

https://doi.org/10.1016/j.cclet.2025.111671
1001-8417/© 2026 Published by Elsevier B.V. on behalf of Chinese Chemical Society and Institute of Materia Medica, Chinese Academy of Medical Sciences.

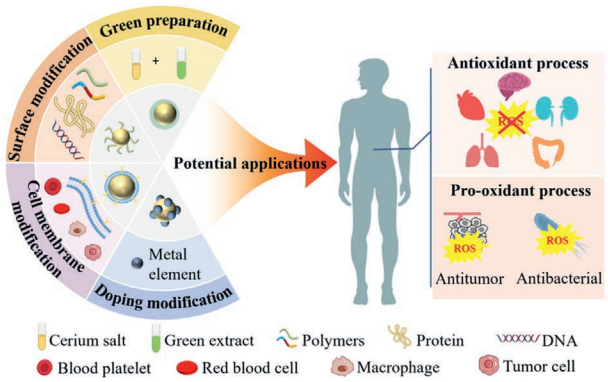


Fig. 1. Schematic diagram of green preparation, surface modification, cell membrane biomimetic modification, doping modification and potential medical applications of CeO_2 NZs.

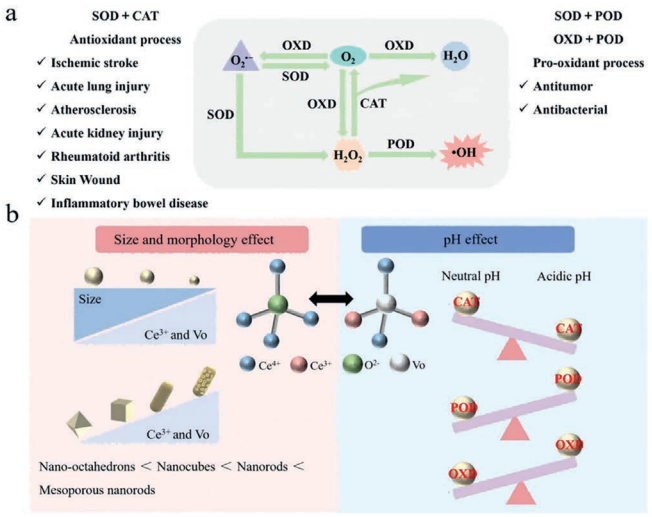


Fig. 2. (a) Schematic diagram of the relevance between multiple mimetic enzyme activities of CeO_2 NZs and the field of biomedicine. (b) Schematic diagram of influence of particle size and morphology of CeO_2 NZs on activity through modulation of reversible cycling between Ce^{3+}/Ce^{4+} and modulation of its mimetic activity by pH.

2. Catalytic properties of CeO_2 NZs and influencing factors

Cerium in CeO_2 exists in two valence states of Ce^{3+} and Ce^{4+} [21]. Due to the reversible cycling between Ce^{4+} and Ce^{3+}, the lattice is prone to oxygen vacancies, which is a key factor in the generation of redox enzyme-mimicking activities [22]. CeO_2 NZs have a variety of enzyme mimetic activities such as superoxide dismutase (SOD), catalase (CAT), oxidase (OXD), POD [23,24]. The four mimetic activities of CeO_2 NZs can be classified into antioxidant and pro-oxidative effects, which can regulate reactive oxygen species (ROS) in the body. This is closely related to the treatment of ROS-related diseases. The relevance between multiple mimetic enzyme activities of CeO_2 NZs and the field of biomedicine as shown in Fig. 2a. SOD- and CAT-mimetic activities exhibiting the antioxidant effect can break down the production of superoxide anions ($O_2^{\bullet-}$) or hydrogen peroxide (H_2O_2) into O_2 and H_2O. The Ce^{3+}/Ce^{4+} ratio displays a significant effect on the SOD- and CAT-mimetic activities of CeO_2 NZs [25,26]. POD- and OXD-mimetic activities perform the pro-oxidant effect that produces ROS to attack pathogens and microbes. Its mimetic enzyme activities are closely related to its own properties and environmental factors. It mainly includes particle size, morphology, pH, temperature, surface modification and doping factors, *etc.* [11]. Among them, surface modification and doping affect the activity by interacting with cerium ions and regulating the electronic structure, producing lattice distortion, respectively [27,28]. This will be described in detail in Sections 4.1 and 4.3. Consequently, this section mainly summarizes the influences of particle size, morphology, pH and temperature.

2.1. Particle size and morphology effect

The effects of particle size and morphology on the catalytic activity of CeO_2 NZs are mediated through the modulation of the Ce^{3+}/Ce^{4+} ratio and oxygen vacancies. As shown in Fig. 2b, as the particle size of CeO_2 NZs decreases, more O^{2-} located in the tetrahedral interstitial positions are released, form more oxygen vacancies to convert Ce^{4+} to Ce^{3+}, providing more active sites for redox reactions to reinforce the catalytic activity [11,29,30]. Generally, the shapes of CeO_2 NZs mainly include nanorods, nano-octahedrons, nanocubes, mesoporous structures, *etc.* CeO_2 nanorods show higher oxygen vacancy content and higher catalytic activity compared to nano-octahedrons and nanocubes [31–33]. Furthermore, the formation of mesoporous structure increases the surface area of CeO_2 NZs. Consequently, more active sites are exposed on the surface and more oxygen vacancies are also formed [34]. Compared to non-porous nanorods, porous CeO_2 nanorods along with more specific surface areas and higher Ce^{3+} content perform stronger POD-mimetic activity [35]. Surface-intrinsic strain in ultrathin CeO_2 nanosheets driven by thickness cutting strengthens the covalent nature of Ce-O bonding, resulting in a greatly enhanced decomposition of $O_2^{\bullet-}$. The Ce^{3+} and oxygen vacancy concentrations are greatly elevate compared to that of the nanocubes [36].

2.2. pH effect

pH is one of the most important environmental factors affecting enzyme activity. As shown in Fig. 2b, CeO_2 NZs have excellent CAT-mimetic activity under neutral conditions. However, excessive H^+ inhibits the conversion of Ce^{4+} to Ce^{3+} under acidic conditions and hinder the decomposition of surface-adsorbed H_2O_2 [37]. This phenomenon might cause cytotoxicity [38]. CeO_2 NZs display higher OXD- and POD-mimetic activities at pH 4.0 whereas the OXD-mimetic activity is significantly reduced at pH 7.0 [39,40]. This pH dependence presents the potential of designing biochemical applications under specific pH conditions, such as releasing drugs or performing bioassays in the acidic conditions in the tumor microenvironment, while protecting cells at physiological pH. It is vitally necessary the pH of the disease microenvironment should be considered to ensure the desired enzymatic activity at the appropriate pH conditions during the design of CeO_2 NZs in therapeutic application.

2.3. Temperature effect

Temperature is an important environmental factor in enzyme activity. However, most of the current studies have focused on exploring the effect of temperature as a synthesis parameter on CeO_2 NZs, while the effect of temperature as an environmental factor on its activities has rarely been reported. SOD-mimicking activity shows a trend of increasing with the rise of temperature in both low-temperature (4, −20 and −80 °C) and high-temperature environments (40–70 °C), and it is significantly higher in the high-temperature environment. Lower temperature has an inhibitory effect on the antioxidant activity, while higher temperature promotes the circulation of cerium ions [41]. In some temperature-sensitive applications, it is necessary to precisely control the environmental temperature to ensure the stable exertion of its activity.

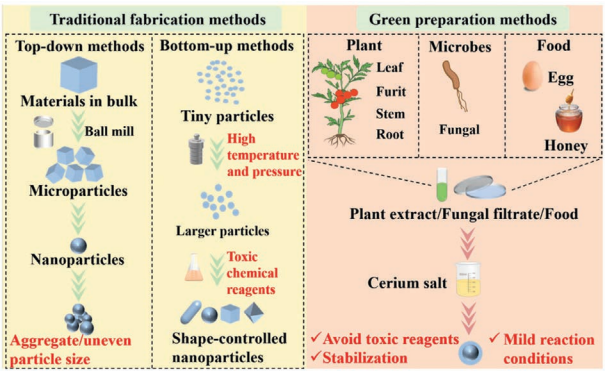


Fig. 3. Traditional and green fabrication methods of CeO_2 NZs.

3. Fabrication of CeO_2 NZs

The effects on the fabrication methods on the catalytic properties of CeO_2 NZs are summarized and compared. Understanding its fabrication process is crucial for optimizing the performance of CeO_2 NZs and expanding their application areas. Fabrication methods of CeO_2 NZs involve traditional and the novel progress of green preparation methods as illustrated in Fig. 3. Due to the instability and the use of toxic chemical reagents in CeO_2 NZs prepared by traditional fabrication methods, this section mainly introduces how green preparation methods to improve these limitations.

3.1. Traditional fabrication methods

Traditional fabrication methods mainly include solid-phase synthesis method, hydrothermal method, sol-gel method, microemulsion method, precipitation method and the further developed ion-assisted sol-gel method [42,43]. Traditional fabrication methods involve the top-down method and the bottom-up method. The top-down method refers to the preparation process of dividing large particles into smaller size particles, such as grinding or high temperature roasting decomposition [44]. The method can avoid the usage of toxic solvents, which is more beneficial for environmental protection. Additionally, the top-down method is simpler and more rapid with lower production cost. However, it is more difficult to accurately control the shape of CeO_2 NZs and the particle size is non-uniform. Besides, it is easier to occur agglomeration [45]. While the bottom-up method is the self-assembly of very smaller atoms to produce larger, more complex NPs. Relatively speaking, the bottom-up method can be used to achieve more controllable shape, higher purity, and uniform particle size of CeO_2 NZs by adjusting the reaction conditions (reactant concentration, reaction temperature and pressure) [44]. The hydrothermal method, one of the bottom-up method, can be used to prepare ultra-small CeO_2 NZs, CeO_2 nanorods, octahedrons and cubes [46–49]. Microemulsion method can prepare CeO_2 NZs with comet-like and prismatic shapes [50]. In addition, the bottom-up method can also prevent particle from agglomeration through the addition of surfactants, stabilizing agents and other substances [51]. However, the bottom-up method often involves the usage of toxic chemical reagents. It is unavoidable for the environment and the human body to be harmed. Consequently, it is vitally necessary to explore green technologies to avoid the disadvantages of traditional fabrication methods for the preparation of CeO_2 NZs and widen its application.

3.2. Green preparation methods

Green preparation methods are simpler, more economical and environmentally beneficial comparing with the traditional methods. Some extracts generated from plants, food even some microbial have been used to prepare CeO_2 NZs as illustrated in Fig. 3. The effects on the formation and properties of CeO_2 NZs have been extensively explored [52].

3.2.1. Plant-mediated green preparation method

Plant-mediated green preparation of CeO_2 NZs is one of the most common methods. The use of plant green extracts without toxic chemicals can present superior biocompatibility. The reaction is simpler, faster, and environmentally friendly with mild conditions. For the preparation of plant-mediated CeO_2 NZs, plant extract is generally prepared by boiling or infusing the plant extracted parts. The extracts are mixed with cerium precursors under stirring and heating condition. The formation, particle size and stability of CeO_2 NZs can be controlled with the assistance of stabilizing effects from plant extracts [52]. In the absence of *Aloe vera* extract, CeO_2 NZs are easily precipitated, presenting the worse stability. While the stable CeO_2 NZs enable to form upon the addition of *Aloe vera* extract [53]. It has been shown plant-mediated CeO_2 NZs exhibit desirable biological activity than plant extracts or CeO_2 NZs alone [54,55]. In the last three years, the plant-mediated preparation of CeO_2 NZs reported have desired antioxidant, antimicrobial, and antidiabetic bioactivities as exhibited in Table 1 [54,56–59]. With the addition of *Manilkara zapota* peel and *Mentha royleana* leaf extract, CeO_2 NZs possess excellent antidiabetic activity, displaying the more desirable inhibitory to α-amylase and α-glucosidase activities [54,57]. Moreover, the green prepared CeO_2 NZs show the largest bacterial inhibition zone as compared to peel extract and CeO_2 NZs. It is also found to be more inhibitory to bacteria than fungi, which may be due to the difference in cell membranes [54]. *Oldenlandia umbellata* leaf extract enable CeO_2 NZs to present better antimicrobial activity at 5 μg/mL compared to other extracts. CeO_2 NZs present dramatic enhancement of antimicrobial activity through green extracts and doping with OsO_4 [59]. *Oroxylum indicum* fruit and *Zingiber officinale* stem extract promote CeO_2 NZs to display better antioxidant activity at lower concentration [56,58].

Most of the current plant-mediated preparation of CeO_2 NZs present a spherical morphology, which might limit CeO_2 NZs to exert better catalytic activity and oxygen storage capacity. The morphology of CeO_2 NZs prepared *via* plant-mediated methods can be affected by doping modification, ionic liquids and plant extract concentration. The non-spherical morphologies of CeO_2 NZs may be due to the lattice distortion caused *via* doping, which affects the morphology and structural features of CeO_2 NZs [60]. Ionic liquids can control the growth and aggregation behavior of CeO_2 NZs. The number and position of anionic and cationic groups control the surface morphology and size [61]. The doping strategies combined with ionic liquids enabled the SrO/CeO_2 and CeO_2/ZrO_2 NZs to present a nanorod structure, endowing them with better activity [61,62]. The concentration of plant extracts also affects the morphology of CeO_2 NZs. As the amount of *aloe vera* gel increased, the morphology of CeO_2 NZs changed from bell-shaped to sea urchin-shaped and then to flower-shaped [63]. This affects the properties of CeO_2 NZs such as specific surface area, porosity and surface energy. In addition, it is a way to direct CeO_2 NZs to form specific structures to control its morphology through using plants as bio-templates method. China rose petal is used as robust bio-template for the facile fabrication of novel ceria nanosheet with a thickness of approximate 7 nm *via* a continuous infiltration process. The morphology of the nanosheets results in a higher Ce^{3+}/Ce^{4+} ratio and more oxygen vacancies [64]. Preparation of non-spherical CeO_2 NZs using adjusted extract concentration, doping, ion liquids and bio-templating strategies is intended for the plant-mediated preparation of CeO_2 NZs with diverse morphology and better performance.

Table 1
Various plants used in the preparation of CeO_2 NZs and its performances.

Plant name	Part	Average size (nm)	Biological evaluation			Ref.
			Antidiabetic	Antimicrobial inhibition zone (mm) [a]	Antioxidant [b]	
Manilkara zapota	Peel	15 ± 2	Inhibition rate of 100 μg/mL CeO_2 NZs: α-amylase (74.13 %) and α-glucosidase (90.61 %)	50 μg/mL CeO_2 NZs: *P. aeruginosa* (33), *Escherichia coli* (31), *S. aureus* (25), *B. subtilis* (23), *A. niger* (21) and *C. albicans* (19)	—	[54]
Oldenlandia umbellata	Leaf	22–24	—	5 μg/mL CeO_2/OsO_4: *K. pneumoniae* (23), *E. coli* (33), *B. subtilis* (26), *S. aureus* (36) and multidrug-resistant *P. aeruginosa* (34)	Inhibition rate of 6 μg/mL CeO_2/OsO_4: DPPH (78 %)	[59]
Mentha royleana	Leaf	46–56	Inhibition rate of 500 μg/mL CeO_2 NZs: α-amylase (~80 %) and α-glucosidase (~45 %)	—	Inhibition rate of 1000 μg/mLCeO_2 NZs: DPPH (31 %), ABTS (46.7 %), ·OH (50 %)	[57]
Oroxylum indicum	Fruit	30	—	—	Inhibition rate of 100 μg/mL CeO_2 NZs: DPPH (63.4 %)	[58]
Zingiber officinale	Stem	3.73	Inhibition rate of CeO_2 NZs: α-amylase (64.1 %)	*E. coli* (7), *P. aeruginosa* (7), *K. pneumoniae* (7), *S. aureus* (7), MRSA (7), *S. entertica* (7)	Inhibition rate of 4 μg/mL CeO_2 NZs: DPPH (34 %), ABTS (43 %)	[56]

[a] *P. aeruginosa*: *Pseudomonas aeruginosa*; *E. coli*: *Escherichia coli*; *S. aureus*: *Staphylococcus aureus*; *B. subtilis*: *Bacillus subtilis*; *A. niger*: *Aspergillus niger*; *C. albicans*: *Canidia albicans*; *K. pneumoniae*: *Klebsiella pneumoniae*; *S. entertica*: *Salmonella enterica*.
[b] DPPH: 2,2-diphenyl-1-picrylhydrazyl; ·OH: hydroxyl radical; ABTS: 2,2′-azino-bis(3-ethylbenzothiazoline-6-sulfonic acid).

3.2.2. Microbes-mediated preparation methods

The abundant secondary metabolites of microorganisms can mediate the green preparation of CeO_2 NZs, presenting excellent stability and dispersion [65]. Fungus secretes large amounts of proteins that can be used to synthesize CeO_2 NZs. The fungal filtrate contains enzymes, anthraquinones that are also responsible for the reduction and stabilization processes [66,67]. Microbes-mediated CeO_2 NZs display a single activity and lower antimicrobial activity compared to that of plant-mediated CeO_2 NZs [65–67]. It is rarely seen microbes-mediated preparation of CeO_2 NZs is reported in recent years. The possible reason may be attributed to more cultivation and maintenance conditions compared to plant preparation methods, which increase the cost and operational complexity.

3.2.3. Food-mediated preparation methods

CeO_2 NZs mediated *via* food have increasingly attracted wide attention [68–71]. The higher amount of carbohydrates, enzymes and vitamins in honey enable to encapsulate and stabilize CeO_2 NZs while inhibit its excessive aggregation or crystal growth [68]. Furthermore, it is noted honey increase in crystallinity of CeO_2 NZs and achieve more uniform in particle size and shape with the increase of calcination temperature. Branched starch contributes to exposure of active sites, the generation of numerous pores and a well-structured surface. Therefore, starch-assisted preparation of CeO_2 NZs presents desirable properties and antimicrobial activity [71]. However, food-mediated preparation of CeO_2 NZs has rarely been reported in recent years. The probable reason may be ascribed to the relatively homogeneous functionality in practical applications, which is mainly focused on antimicrobials.

4. Modification strategies of CeO_2 NZs

After summarizing and discussing the traditional and green preparation methods of CeO_2 NZs, deep understandings have been gained regarding how the choice of preparation methods can enhance the performance of CeO_2 NZs. To further increase the potential of CeO_2 NZs for clinical applications, it is also necessary to analyze the properties of CeO_2 NZs from an application perspective. CeO_2 NZs have been extensively studied in the biomedical field due to its antioxidant and pro-oxidant properties. However, the interactions among enzyme activities, the susceptibility to agglomeration, toxicity and nonspecific targeting issues are found [19,45,72–76]. It is of great importance to take effective measures to ameliorate the deficiency *via* modification and strengthen the original properties. Surface modification on CeO_2 NZs has the effect of preventing agglomeration and improving biocompatibility [27]. Cell membrane biomimetic modification primarily confers CeO_2 NZs targeting properties [77]. The doping strategy reinforces the multi-enzyme-like activity of CeO_2 NZs and improves the enzyme selectivity in specific environments [78,79], even enables applications in sensing capability [80,81].

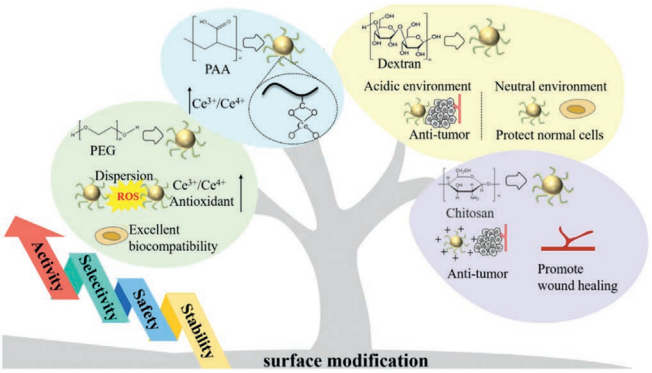


Fig. 4. Commonly used surface modification materials and their enhancement of CeO_2 NZs properties.

4.1. Surface modification on CeO_2 NZs

Generally, the catalytic reactions occur on the surface of CeO_2 NZs. The surface modification alters the surface physicochemical properties of CeO_2 NZs, which in turn reinforces the stability and modulates catalytic activity as established in Fig. 4. Among them, materials such as polyethylene glycol (PEG), polyacrylic acid (PAA), dextran and chitosan are introduced due to their better biocompatibility and easier surface modification ability [82].

4.1.1. Surface modification from synthetic polymers

Due to the multivalent binding effect, the polymer has tighter adsorption properties, giving CeO_2 NZs better colloidal stability and dispersion [17]. After being PEG modification, the agglomerated CeO_2 NZs are dispersed among each other, showing excel-

lent stability in a range of physiological solutions including water, cell culture media and serum [83]. The modification from synthetic polymer can reinforce the biocompatibility of CeO_2 NZs [83–85]. The survival rate of normal human hepatocytes (L-02) at 50 μg/mL concentration of CeO_2 NZs is only 36.7 %, while the survival rate at the same concentration of PEG-CeO_2 NZs is ~83 % [83]. No cytotoxicity to human osteoblasts (SAOS-2) when the concentration of PAA-CeO_2 NZs is 500 μg/mL [84]. Additionally, the interaction between polymers and CeO_2 NZs alter the chemical environment on the surface of CeO_2 NZs, making it easier for Ce^{4+} to be reduced to Ce^{3+}. Compared to CeO_2 NZs, PEG-modified CeO_2 NZs present higher Ce^{3+}/Ce^{4+} ratio, which result in elevated SOD2 protein expression in normal hepatocytes (L-02 cells) and more effectively protected normal cells from ROS damage [83]. At higher temperatures, the conformation of PAA change from a curled to a stretched structure, which provided more carboxylate-anchored localization sites on the CeO_2 surface along with an increase of Ce^{3+} concentration. Conversely, the sequence result leads to a gradual increase in the SOD and POD-mimetic activities as well as a gradual decrease in the CAT and OXD-mimetic activities [84].

4.1.2. Surface modification from natural polymers

It is well-known natural polymers are extremely abundant. They possess superior biological activity and have been used for surface modification of CeO_2 NZs. In contrast to the synthetic polymers which require bridging molecules. The hydroxyl groups of natural polymers can interact with the CeO_2 surface in a variety of ways, contributing to the formation of stronger encapsulation layers than synthetic polymers [27]. The performance enhancement of CeO_2 NZs through the modification of various natural polymers are shown in Table S1 (Supporting information) [86–93]. Surface modification of natural polymers accelerates the biocompatibility of CeO_2 NZs. The concentration of non-toxic upon cells reaches 1000 μg/mL [88,89]. Natural polymers themselves also have biological functions endowing some specifical bind properties of the receptor to elevate the active targeting of CeO_2 NZs [88,93]. Dextran can bind to scavenger receptors at the site of inflammation, facilitating dextran-CeO_2 NZs in inflammatory bowel diseases. Fluorescently labeled dextran-CeO_2 NZs emerging the fluorescence signal is mainly concentrated in the gastrointestinal tract. The fluorescence signal is more significant in colitis mice. This further proves that dextran modification enables CeO_2 NZs to specifically target the inflammatory site [88]. In the treatment of atherosclerosis, hyaluronic acid-CeO_2 NZs actively target plaque-associated macrophages in atherosclerosis to remove excess ROS. In atherosclerotic mice, the fluorescence intensity of hyaluronic acid-CeO_2 NZs in the aorta is approximately 3-fold stronger than injected with free fluorescent dye. Meanwhile, it shows higher plaque-targeting behaviors than the poly-aspartic acid-coated CeO_2 NZs. It is due to hyaluronic acid-CeO_2 NZs are rapidly endocytosed by macrophages or endothelial cells in the aorta in plaques and tend to accumulate in plaques [93].

Some natural polymer-modified CeO_2 NZs can exhibit pH-dependent antioxidant/pro-oxidant activity. This property protects normal cells from free radical damage at physiological pH, but produces a pro-oxidant killing effect on cancer cells in acidic environments [86,87,91]. Dextran-CeO_2 NZs have antioxidant properties at pH 7.0 and the highest destructive effect on cancer cells at pH 6.0, which offers potential applications for cancer therapy [87]. This pH-dependent change in activity serves natural polymer-modified CeO_2 NZs the potential for a wider range of applications in different biological environments.

The surface modification from natural polymer increases the biocompatibility and stability of CeO_2 NZs. Mimetic enzyme activity and pH-dependent antioxidant/ pro-oxidant activity are also strengthened. It is found that the thickness of polymer modification is one of the important factors affecting the catalytic activity, stability, and cellular uptake of the modified CeO_2 NZs. The thinner coating promotes faster substrate transfer to the CeO_2 NZs core, which in turn exerts stronger catalytic activity [39]. The thinner surface modification maintains competitive colloidal stability and antioxidant activity of CeO_2 NZs, further boost the recycling ability of CeO_2 NZs [94]. Subsequently, adjusting the thickness of the surface coating can be optimized for biomedical applications of CeO_2 NZs. In the future, it is necessary to combine various characterization methods to explore the surface interaction and the binding mechanism between polymers and CeO_2 NZs.

4.2. Cell membrane biomimetic modification on CeO_2 NZs

Polymer modification on CeO_2 NZs lacks targeting ability, which might trigger an immune response in the body. The risk of clearance is increased through the immune system [95]. Nevertheless, the ability of natural cell membranes endowing more prolonged circulation time, being immune escape, and targeting facilitates the application of membrane coating technology in CeO_2 NZs delivery as shown in Table S2 (Supporting information) [16,18,96–103]. It is key that the membrane coating is structurally and functionally similar to the host cell. Introduced cell membrane proteins bind to specific receptors expressed on the surface of target cells for precise delivery of CeO_2 NZs [77,101]. Under inflammatory conditions, intercellular adhesion molecule-1 (ICAM-1) expression on alveolar epithelial cells is upregulated, while macrophage-1 antigen (MAC-1) on macrophage membranes can specifically bind to ICAM-1 [104,105]. Macrophage membrane-coated CeO_2 nanocomplexes incubate with inflammatory cells show stronger fluorescence compared to that of PEG modification. The blockade of the ICAM-1 binding site causes a significant decrease in the level of binding capacity [101]. Platelet membrane-coated CeO_2 NZs emerge higher uptake rates in lipopolysaccharide-stimulated RAW264.7 cells and higher accumulation in the aorta than uncoated CeO_2 NZs, achieving dual targeting of atherosclerosis [99]. Glycoprotein IIb (GPIIb) and P-selectin (CD62p) expressing on platelet membranes can aggregate and activate more platelets to accelerate wound healing. The platelet membrane-coated CeO_2 NZs obviously enhance platelet adhesion to collagen. Meanwhile, it shows a mean rate of platelet aggregation of 16.7 % ± 1.3 % [98]. As adhesion molecules are expressed on homologous tumor cell membranes, corresponding cancer cell membrane-coated CeO_2 NZs is endowed with homologous recognition and homing properties *via* receptor-ligand binding. MDA-MB-231 cancer cells subjected to membrane-encapsulated CeO_2 nanocomplexes show higher fluorescence intensities, which is highly higher normal cells, suggesting that membrane encapsulation remarkably increases the intracellular uptake of the nanocomplexes [97]. The obvious advantages of cell membranes-coated CeO_2 NZs and the abundant source of cell membranes provide a solid foundation for its individualized precision medicine.

4.3. Doping modification on CeO_2 NZs

Surface modification and cell membrane biomimetic modification strategies play an important role in improving the biocompatibility, stability and targeting of CeO_2 NZs. To further optimize the catalytic performance and enzyme mimetic activity, other modification approaches are also extensively explored. Doping modification strategies can be used to modulate the physicochemical properties of CeO_2 NZs by introducing other elements to achieve finer regulation of the CeO_2 NZs' performance.

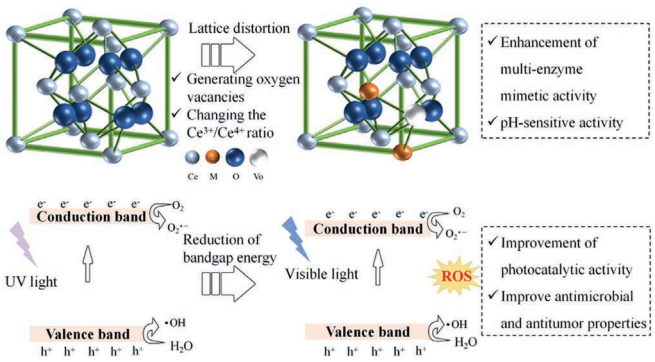


Fig. 5. Doping-induced changes in CeO_2 NZs lattice and photocatalytic activity of metal-doped CeO_2 NZs.

4.3.1. Transition metals doped CeO_2 NZs

Transition metal doping has achieved the dual mechanism of modulating the electronic structure of CeO_2 and generating lattice distortion (Fig. 5). Through doping modification, the band gap energy of CeO_2 NZs can be lowered to absorb visible light and generate photogenerated electron-hole pairs, which participate in redox reactions to generate ROS. Doped transition metal CeO_2 NZs exhibit enhanced antibacterial and antitumor capacity in comparison to that of undoped CeO_2 NZs [106–108]. Moreover, different valence states can provide different reactive centers of activity, elevating the catalytic selectivity of specific reactions [109].

The multi-enzyme activities of CeO_2 NZs are effectively reinforced by Cu doping. The selective regulation of these activities has been realized in specific environments. The OXD and POD-mimetic activities of Cu-CeO_2 NZs are optimal at pH 3.5 and 4 condition. The CAT activity is excellent while the OXD and POD-mimetic activities are weakest at pH 6.5. At the pH 6.5 tumor microenvironment, the CAT-mimetic activity is unaffected through the activities of the other two mimics and alleviated the hypoxic condition of tumor cells [78]. POD activity is boosted and hydroxyl radical antioxidant capacity activity is inhibited whereas the antimicrobial effect is improved through modulating the electronic structure of CeO_2 NZs and influencing the kinetics of the catalytic reaction [19].

Co-CeO_2 NZs have a unique role in biosensing and detection due to its superior POD-mimetic activity. It is active under acidic conditions, which hinder *in vivo* sensing applications. It is demonstrated the affinity of CeO_2 NZs for H_2O_2 and 3,3′,5,5′-tetramethylbenzidine (TMB) is distinctly increased through the introduction of Co. The catalytic efficiency is dramatically reinforced compared with that of the undoped CeO_2 NZs at pH 6.0 [110]. The Co-CeO_2 NZs enable to mimic POD activity in a neutral pH environment, accompanying with different oxidative enzymes. This is beneficial to more effectively catalyze the generation of POD activity, enabling the detection of specific biomarkers (*e.g.*, glucose, galactose, cholesterol). Ultrasmall Co-CeO_2 nanodots are prepared and uniformly dispersed in mesoporous silica to form mesoporous spheres. The excellent POD-mimetic catalytic ability and mesoporous structure of Co-CeO_2 have achieved the quantitative assessment of cellular glutathione levels, providing a potential analytical tool for clinical diagnosis [80].

4.3.2. Alkaline-earth metals doped CeO_2 NZs

The doping of alkaline earth metals changes the electronic structure and band gap size of CeO_2 NZs, which can promote more electrons to convert to the conduction band and generate electron-hole pairs. The electrons generated by the excitation react with O_2 dissolved in water to form $O_2^{\bullet-}$, and the holes react with water molecules to form $^{\bullet}OH$. The effects of Mg, *Ca*, Sr and Ba doping on CeO_2 NZs are detected [28]. The reduced grain size of Ba doped CeO_2 NZs, making it easier to penetrate the bacterial cell membrane. Ba ions act as electron traps to reduce electron-hole pair complexation and increase oxygen vacancies, promoting ROS formation. The result presents the most excellent antibacterial activity.

4.3.3. Intercomparison of doping strategies

Doping transition metal can generate active sites and promote catalytic reaction kinetics. It can adjust the electronic structure of CeO_2 NZs and control the oxygen vacancy density. It is important to enhance the multi-enzyme selectivity of CeO_2 NZs. The transition metal doping also induces the enzyme mimicking activity of CeO_2 NZs to produce special pH selectivity. It is conducive to break the pH limitation of CeO_2 NZs mimicking enzyme activity in some disease microenvironments. The doping strategies widely broadens CeO_2 NZs application in disease treatment and sensing. Alkaline earth metal ion doping acts as an electron trap which can lead to a change in the band gap energy and slow down the electron-hole pair complexation. This change promotes the generation of ROS which is suitable for antibacterial and antitumor applications. Despite the many advantages of doping modification, some potential risks should not be ignored. For example, Mn-doped CeO_2 NZs show 13 times higher POD-mimetic activities than pure CeO_2 NZs [111]. Concerns remain about whether the excessive generation of free radicals may induce toxicity to cells *in vivo*. Therefore, it is necessary to focus on the balance between activity and safety.

4.4. Biosafety comparison of modification strategies

To extensively widen the application of the three modification strategies in the clinical transformation of CeO_2 NZs, the biosafety of the three modification methods is summarized from four aspects: cytotoxicity, hemolysis, animal blood routine indexes and biochemical indexes in Table 2 [16,19,83,84,88–90,96,99,102,103,107,112]. Most of the three modification strategies are no cytotoxic along with the cell viability beyond 80 % at concentrations of 100 or 200 μg/mL. Especially the natural polymer-modified CeO_2 NZs remains non-cytotoxic even at high concentrations. Dextran and cellulose-modified CeO_2 NZs are safer at high concentrations compared to that of other modification methods. CeO_2 NZs tends to accumulate in the liver and spleen [113]. It is also vitally important to note that cytotoxicity experiments with CeO_2 NZs should examine the viability of normal liver, spleen and lung cell lines in addition to the selection of disease-related cell lines. In terms of hemolysis, available data indicate that CeO_2 NZs with cell membrane biomimetic modification have a hemolysis rate of <5 %, indicating preferable blood compatibility. The use of clinical assays to characterize the biosafety of CeO_2 NZs promotes its clinical relevance. None of the indexes present in the Table 2 are significantly different from healthy mice. The natural polymer surface modification and cell membrane biomimetic modification CeO_2 NZs have superior *in vivo* biosafety. Although there are no significant differences, the cell membrane mimetic modifications still show elevated aspartate aminotransferase (AST), alkaline phosphatase (ALP) and blood urea nitrogen (BUN). This phenomenon reminds us it is highly necessary to focus on the status of liver and kidney functions after administration CeO_2 NZs involving its modification compounds. Overall, natural polymer surface modification and cell membrane biomimetic modification strategies behave better biosafety. For doping strategies, the current explorations about *in vivo* safety are bare and still need to be focused in the future.

5. Potential clinical applications

The three strategies provide a solid foundation for the usage of CeO_2 NZs in biomedical applications. The section focuses

Table 2
Comparison of cytotoxicity, hemolysis rates, animal blood routine indexes and biochemical indexes of three modification strategies.

Modification strategy	Cytotoxicity			Hemolysis	Animal level indicator		Ref.
	Cell type [a]	Concentration	Cell viability		Blood routine index [b]	Biochemical index [c]	
PEG modification	L-02 cells	50 μg/mL	CeO_2 NZs (36.7 %); PEG-CeO_2 NZs (~80 %)	—	—	—	[83]
PAA modification	Saos-2 cells	100 μg/mL	PAA-CeO_2 NZs (>100 %)	—	—	—	[84]
Dextran modification	NIH3T3 cells	1000 μg/mL	Dextran-CeO_2 NZs (>80 %)	—	RBC (~8.5×10^{12}/L), WBC (~6×10^9/L), LYM (~4×10^9/L), neutrophil (~3×10^9/L), PLT (~240×10^9/L), HGB (~120 g/L)	ALT (~40 U/L), AST (~200 U/L), UREA (~20 μmol/L), CREA (~20 μmol/L), LDH1 (~19 U/L), CK (~3000 U/L)	[88]
Chitosan modification	HFF cells	200 μg/mL	Chitosan-CeO_2 NZs (99.82 %)	—	—	—	[90]
Cellulose modification	HeLa cells	1000 μg/mL	Cellulose-CeO_2 NZs (~90 %)	—	—	—	[89]
Red blood cell membrane modification	HK-2 cells	200 μg/mL	Modified CeO_2 NZs (~100 %)	~2.5 %	—	ALT (~21 U/L), AST (~110 U/L), BUN (~6.5 mmol/L), TP (~50 g/L)	[16]
Macrophage cell membrane modification	RAW264.7, HUVECs, Chondrocyte	200 μg/mL	Modified CeO_2 NZs (~80 %)	<0.1 %	MCV (~44 fL), MPV (~6.5 fL), RBC (~10×10^{12}/L), UREA (~9 mmol/L)	ALB (~30 g/L), ALP (~18 U/L), BUN (~25 mmol/L), ALT (~50 U/L)	[103]
Platelet membrane modification	HUVECs	200 μmol/L	CeO_2 NZs (~87 %), Modified CeO_2 NZs (~125 %)	1.29 %	PLT (~1.1×10^9/L) WBC (~2×10^9/L), RBC (~8×10^{12}/L), HGB (~112 g/L)	ALT (~22 U/L), AST (~125 U/L), BUN (~4.4 mmol/L), CREA (~70 μmol/L), HDL (~1.3 mmol/L), LDL (~4 mmol/L), TC (~12 mmol/L), TG (~1.4 mmol/L)	[99]
HeLa cervical cancer cells membrane modification	HeLa cells	200 μg/mL	Modified CeO_2 NZs (~10 %)	~0.5 %	——	ALT (~20 U/L), AST (~38 U/L), BUN (~8 mmol/L), TP (~68 g/L), ALB (~38 g/L)	[102]
Apoptotic chondrocytes membrane	RAW264.7, HUVECs, Chondrocyte	200 μg/mL	Modified CeO_2 NZs (~95 %)	<2 %	RBC (~8×10^{12}/L), WBC (~7×10^9/L), LYM (~3.8×10^9/L), HCT (~38 %), PLT (~1200×10^9/L), HGB (~100 g/L)	ALT (~26 U/L), AST (~170 U/L), CREA (~14 μmol/L), ALP (~100 U/L)	[96]
Cu-doped CeO_2 NZs	hGF cells, hPDLSc cells	200 μg/mL	Cu-doped CeO_2 NZs (~98 %)	——	RBC (~11×10^{12}/L), WBC (~8×10^9/L),	——	[19]
Zn-doped CeO_2 NZs	HepG2 cells	100 μg/mL	Zn-doped CeO_2 NZs (~74 %)	——	——	——	[112]
Pd-doped CeO_2 NZs	NIH3T3 cells	250 μg/mL	Pd-doped CeO_2 NZs (~90 %)	——	——	——	[107]

[a] L-02 cells: human normal liver cells; Saos-2 cells: human osteosarcoma cell line; NIH 3T3 cells: mouse embryonic fibroblast cells; HFF cells: human foreskin fibroblast cells; HeLa cells: human cervical cancer cell line; HK-2 cells: human renal cortical proximal tubular epithelial cells; RAW264.7: mouse monocyte macrophage leukemia cells; HUVECs: human umbilical vein endothelial cells; Chondrocyte: cartilage cells; hGF cells: human gingival fibroblasts; hPDLSc cells: human periodontal ligament stem cells. HepG2 cells: human hepatocellular carcinoma cells.

[b] RBC: red blood cell; WBC: white blood cell; LYM: lymphocyte; PLT: platelets; HGB: hemoglobin; MCV: mean corpuscular volume; MPV: mean platelet volume; HCT: hematocrit.

[c] ALT: alanine aminotransferase; UREA: urease; CREA: creatinine; LDH1: lactate dehydrogenase; CK: creatine kinase; TP: total protein; ALB: albumin; HDL: high density lipoprotein; LDL: low density lipoprotein; TC: total cholesterol TG: triglyceride.

on the potential clinical applications of CeO_2 NZs, exploring how these high-performance CeO_2 nanocomplexes to preferably meet the challenges of a wide range of diseases. The concerns are addressed to facilitate their clinical translation. Potential therapeutic effects of CeO_2 NZs exist for ischemic stroke, Alzheimer's disease (AD), acute lung injury, atherosclerosis, acute kidney injury, inflammatory bowel disease, osteoarthritis and skin wounds [6,13]. The potential mechanisms are illustrated in Fig. 6. The representative researches in latest three years are summarized in Table 3 [96,99,101,114–128].

5.1. Diseases of the nervous system

In the treatment of neurological disorders, nanomaterials emerge as attractive candidates for drug delivery across the blood-brain barrier [129,130]. In most studies, the design using targeted modification of CeO_2 NZs and combined application of neuroprotective agents [119,120]. Even at low concentrations, nearly 90 % of free radicals is inhibited. Interestingly, the integrity of the blood-brain barrier still maintained along with reducing the area of cerebral infarction, and restoring neurological function [119,120]. AD requires multi-targeted therapy. CeO_2 NZs are often used in combination with Aβ aggregation inhibiting drugs and hyperphosphorylation of Tau proteins [116,123,131–133].

5.2. Diseases of the respiratory system

Nano-system by co-delivery strategy using the synergistic effect of CeO_2 NZs and drug is designed to reduce inflammation and alleviate pulmonary edema induced through acute lung injury [117].

Table 3
Representative studies on the potential applications of CeO_2 NZs for the treatment of diseases.

Potential application	Modification and synergy [a]	Antioxidant: free radical scavenging	*In vivo* model and administration route[b]	Safety	Clinical perspective	Ref.
Ischemic stroke	DSPE-PEG_{2k}-TPP modified: elevate targeting; ROF: repair damaged nerves	Inhibition rate of 2 μg/mL; TPP@(CeO_2+ROF): $ABTS^{+\bullet}$ (~90 %), $^{\bullet}OH$ (~90 %)	MCAO-induced ischemic stroke, SD rats; i.v.	Metabolized within 14 days	Multi-stage interventions for disease progression	[120]
	PEG modified: prolong cycle time; NBP: repair damaged nerves	Inhibition rate of 0.96 μg/mL NBP-CeO_2 NPs: $ABTS^{+\bullet}$ (~90 %), $^{\bullet}OH$ (~98 %)	MCAO/R-induced ischemic stroke, C57BL/6 mice; i.v.	No toxicity seen after 14 days	Acts at different stages of the disease	[119]
AD	MSN: load composition; curcumin: inhibit Aβ aggregation, antioxidant; IR780: photosensitizer Immobilized; peptide K: targeted	NIR+CICe@M-K: the fluorescence intensity of the ROS probe was significantly reduced	APP/PS1 CE mice; i.v.	No toxicity seen after 30 days	Multi-targeted therapy	[123]
	Resveratrol: antioxidant; Lactoferrin-modified: elevate targeting and biocompatibility	LMC-RES: GSH (3.2-fold) and SOD (2.9-fold) compared to controls	AD, 5xFAD mice; i.v.	No toxicity seen after 8 weeks	Improve the bioavailability of resveratrol	[116]
Acute lung injury	Curcumin: anti-inflammatory and antioxidant	2 μg/mL CeO_2 demonstrate significant $ABTS^{+\bullet}$ scavenging activity	LPS-derived acute lung injury, C57BL/6 mice; tracheal nebulization	No toxicity seen after 14 days	Improving the bioavailability of curcumin	[117]
	Macrophage membranes: boost targeting, fluorescent probe T-TF: imaging	Inhibition rate of HCe-TTF@M (at 100 μg/mL of CeO_2): $^{\bullet}OH$ (73 %), H_2O_2 (~90 %), $O_2^{\bullet-}$(60 %)	LPS-derived acute lung injury, BALB/c mice; inhalation	Clear in 7 days, no toxicity seen at 48 h (blood, organs)	Real-time diagnosis and intervention	[101]
Respiratory syncytial virus infection	—	25 μg/mL Cubic CNPs-processed ROS: 2×10^5 RFU/mg protein	RSV line 19 virus-infected BALB/cJ mice; intranasal instillation	—	Early intervention	[122]
Atherosclerosis	Platelet membranes: improve targeting	Inhibition rate of PCZ@PB NCs: $O_2^{\bullet-}$ (80 %) within 24 h	High-fat diet fed, $ApoE^{-/-}$ mice; i.v.	No toxicity seen after 2 months	Efficient drug delivery	[99]
	Macrophage exosomes: carrier, targeted; SNHG12 gene: repair endothelial cell	Ability to remove $^{\bullet}OH$ and $O_2^{\bullet-}$	High-fat diet fed, $ApoE^{-/-}$ mice; i.v.	No toxicity seen after 14 days	Precision therapy	[125]
Inflammatory bowel disease	Eudragit S100 encapsulated: protects CeO_2 and reduce non-specific distribution	Inhibition rate of 20 μg/mL CeO_2@S100: $O_2^{\bullet-}$ (~60 %)	DSS-induced inflammatory bowel disease, BALB/c mice; oral administration	No toxicity seen after 10 days	Multi-targeted therapy	[118]
	Eudragit S100: protects CeO_2 and reduce non-specific distribution; dextran sodium sulfate: boost targeting	Inhibition rate of TJ-5/DSS/MCN: $^{\bullet}OH$ (~30 %), H_2O_2 (~65 %)	DSS-induced inflammatory bowel disease, BALB/c mice; oral administration	No toxicity seen after 10 days	Dual-targeted and synergistic therapy	[121]
Acute kidney injury	Citric acid modification: elevate stability	Inhibition rate of 400 μg/mL CeO_2: $^{\bullet}OH$ (~40 %), $O_2^{\bullet-}$ (~80 %), $ABTS^{+\bullet}$ (~90 %)	Iohexol-induced acute kidney injury, KM mice; i.v.	No toxicity seen after 21 days	Early diagnosis	[115]
	PEG-folic acid conjugate modification: improve targeting	Inhibition rate of 1 μg/mL Ce-FA: H_2O_2 (65 %), $O_2^{\bullet-}$ (70 %)	LPS-derived acute kidney injury, C57BL/6 mice; i.v.	Largely metabolized after 48 h	Suitable for diseases associated with hypoxia	[124]
Urinary tract infection	Dextran modification: anti-adhesion	Inhibition rate of 100 μg/mL DEC70: DPPH (~60 %), $ABTS^{+\bullet}$ (~45 %)	*E. coli* CFT073-derived urinary tract infection, C57BL/6 J mice; i.v.	DEC10 can be metabolized out of the body within 4 h	Suitable for many conditions of urinary tract infections	[126]

(*continued on next page*)

Table 3 (*continued*)

Potential application	Modification and synergy [a]	Antioxidant: free radical scavenging	*In vivo* model and administration route[b]	Safety	Clinical perspective	Ref.
Osteoarthritis	Apoptotic chondrocyte membranes: boost targeting Dexamethasone: anti-inflammatory	0–100 μg/mL DEX@HMCeNs@M: the UV–visible absorption peaks of DPPH, $ABTS^{+\bullet}$ and $^{\bullet}NO$ are reinforced	MIA-induced osteoarthritis, SD rats; intra-articular injection	No toxicity seen after 24 days	Prolongs drug retention time	[96]
	Fe_2O_3 NPs microspheres: promote cartilage regeneration Hydrogel formation by thiol-modified type I collagen	Inhibition rate of CSH–CeO_2-pFe_2O_3 hydrogels containing 0.5 mmol/L CeO_2: DPPH (~14.5 %)	Bone-deficient, SD rats; intra-articular injection	No toxicity seen after 8 weeks	Intelligent response	[114]
Cutaneous wounds	Fibrous scaffold of *Bletilla striata* polysaccharide/poly(lactic-*co*-glycolic acid) Epidermal growth factor: accelerate wound healing	Inhibition rate of EBCP: $^{\bullet}OH$ (~65 %), H_2O_2 (~60 %), DPPH (~75 %)	Full-thickness skin injury, SD rats; topical treatment	No toxicity seen after 10 days	Promoting wound healing in multiple ways	[127]
	γ-PGA-SH and AM as hydrogel matrices Vancomycin: antimicrobial	Inhibition rate of PACV: $^{\bullet}OH$ (~80 %)	STZ-induced diabetic wound, SD rats; topical treatment	No toxicity seen after 14 days	Promoting wound healing in multiple ways	[128]

[a] DSPE-PEG_{2k}: bis(1,2distearoyl-*sn*–glycero-3-phosphoethanolamine)-*N*-[(poly(ethylene glycol))-2000; TPP: triphenylphosphine; ROF: roflumilast; MSN: mesoporous silica NPs; NBP: Dl-3-*n*-butylphthalide; T-TF: a highly fluorescent NIR-II AIE luminogens; SNHG12 gene: small nucleolar RNA host gene 12 Gene; TJ-M2010–5: a small molecule inhibitor of MyD88; γ-PGA-SH: thiol groups grafted onto poly-γ-glutamic acid; AM: acrylamide.

[b] MCAO: middle cerebral artery occlusion; intravenous injection: i.v.; SD: Sprague-Dawley; MCAO/R: middle cerebral artery occlusion/recanalization; APP/PS1: amyloid beta precursor protein/presenilin 1; LPS: lipopolysaccharide; ApoE: apolipoprotein E; DSS: dextran sodium sulfate; MIA: monoiodoacetate; STZ: streptozotocin.

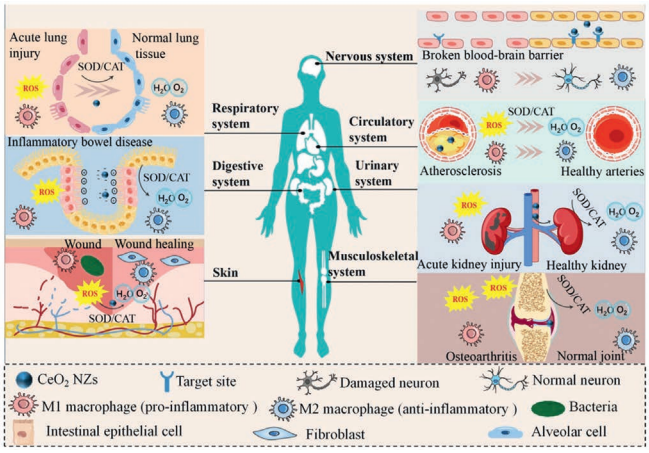


Fig. 6. Mechanisms related to the antioxidant effect of CeO_2 NZs for potential clinical applications utilizing SOD and CAT-mimetic activity. In nervous system, CeO_2 NZs can easily penetrate the blood-brain barrier, exerting antioxidant and anti-inflammatory effects to repair damaged neurons and the blood-brain barrier. For the respiratory system, CeO_2 NZs can catalyze the consumption of many types of ROS, thereby reducing the inflammation of acute lung injury. For the circulatory system, CeO_2 NZs can relieve atherosclerosis-induced oxidative stress, inflammation and remove plaque. For the urinary system, the smaller size of CeO_2 NZs can target the kidneys, relieve oxidative stress and inflammation and repair the damaged kidneys. For the digestive system, CeO_2 NZs can electrostatically target positively charged intestinal tissues through surface modification, thereby scavenging ROS and alleviating inflammation. For the skeletal system, CeO_2 NZs can scavenge ROS and reduce inflammation, which in turn repairs damaged bone tissue. For skin wounds, CeO_2 NZs scavenge ROS and reduce inflammation through antioxidant action, while also acting as a pro-oxidant to kill bacteria, ultimately promoting tissue regeneration.

The wide distribution of CeO_2 NZs *in vivo* and the lack of tracking imaging tools after administration usually lead to adverse effects and impaired therapeutic efficacy. Therefore, studies have developed strategies to accurately monitor and control the distribution of CeO_2 NZs *in vivo* [101]. It is rarely reported CeO_2 NZs treatment of respiratory syncytial virus infection. The therapeutic effect is mainly related to the shape of the CeO_2 NZs. Cubic CeO_2 NZs are superior to spherical CeO_2 NZs in reducing both ROS levels and M1 macrophages [122].

5.3. Diseases of the circulatory system

The formation of atherosclerosis is primarily due to ROS that contribute to the oxidation of low-density lipoprotein (LDL) to Ox-LDL. The process exacerbates the inflammatory response [134]. Majority of the current CeO_2 nanocomplexes have been modified through cellular engineering to target atherosclerotic plaques. It can inhibit the generation of ROS and foamy macrophages to repair the endothelial cells. This approach also boosts biosafety [99,125].

5.4. Diseases of the digestive system

Generally, the tissues are positively charged due to the large amount of eosinophil cationic proteins and transferrin in the colonic tissues of inflammatory bowel disease patients [135]. Most of CeO_2 NZs for the treatment of inflammatory bowel disease are prepared based on the electrostatic targeting, *via* coating with negatively charged HA, PAA, or assembled by growing CeO_2 NZs *in situ* on negatively charged montmorillonite [136–138]. Because of the susceptibility of drugs degradation through gastric acid in the stomach, CeO_2 NZs can be delivered by coated with enteric material or encapsulated in hydrogel carrier to acquire ideal healing effect [88,118,121].

5.5. Diseases of the urinary system

It is easier for ultra-small CeO_2 to pass through glomerular filtration and act directly on renal tubules to reduce oxidative stress and inflammatory response, and then protect renal function [115]. From the perspective of alleviating renal hypoxia, CeO_2 nanocomplexes can produce O_2 through decomposing ROS and reducing

xanthine oxidase activity [124]. CeO_2 NZs modified with glucose as an anti-adhesion component effectively scavenge ROS and restrain FimH-mediated bacterial adhesion for effective treatment of urinary tract infections [126].

5.6. Diseases of the musculoskeletal

Drugs entering the joint cavity are rapidly eliminated through the synovial lymphatic and vascular systems of the joints [139]. CeO_2 NZs coated with apoptotic chondrocyte membranes enhances the localization and retention in the cartilage and facilitates the action of CeO_2 NZs [96]. Encapsulation of CeO_2 NZs in hydrogels can boost lubrication, protect damaged joints and promote cartilage regeneration [114]. CeO_2 NZs are often used in combination with substances to protect cartilage, promote bone regeneration or being used as carriers for the delivery of anti-rheumatic drugs for the treatment of rheumatoid arthritis [140,141].

5.7. Skin

Skin wounds are usually divided into acute and chronic categories [142]. The wound healing process mainly consists of four stages: hemostasis, inflammation, proliferation and remodeling. Excessive release of ROS give rise to persistent inflammation and the formation of chronic wounds [143]. Most studies focus on the scaffolds and dressings containing CeO_2 NZs. The fibrous scaffolds containing epidermal growth factors and CeO_2 NZs is prepared through electrostatic spinning technology [127]. The advantage of CeO_2 NZs composite hydrogel as wound dressing lies in strong antioxidant capacity and tissue regeneration promoting function. Moreover, its three-dimensional porous structure can be long-lasting slow release of CeO_2 NZs synergizing with the wetting, mechanical barrier effect and anti-inflammatory properties of the hydrogel to achieve multi-effective and synergistic treatment of wound repair [128,144,145]. Green synthesis of CeO_2 NZs in bacterial cellulose-based composite films is fabricated using curcumin as precipitant. Focus on the application of CeO_2 NZs as an antimicrobial agent in wounds. The nanocomposite membranes exhibit the most significant antibacterial activity against *E. coli* and *B. subtilis* while maintaining superior cytocompatibility [146]. CeO_2 NZs appear a desirable UV shielding effect. Utilizing natural kaolin nanotubes control the growth of CeO_2 NZs which provides excellent UV protection for the skin [147]. However, it still lacks more systematically specific studies on skin UV protection.

5.8. Antimicrobial applications

Bacterial infections are characterized by higher morbidity and mortality. CeO_2 NZs adsorb to the cell membrane of bacteria *via* electrostatic attraction, which causes the cell membrane to rupture, leading to leakage of cell contents [148,149]. The generation level of ROS can be increased due to the POD- and OXD-mimetic activities of CeO_2 NZs. ROS can reduce the fluidity of cell membrane, which further exacerbate cell membrane damage, alter the structure and function of proteins and DNA as well as cause the death of bacterial. The modification of CeO_2 NZs can further boost the ability to kill drug-resistant bacteria. Cu-doped CeO_2 have displayed almost complete sterilization of multiple-resistant *Staphylococcus aureus* (MRSA) and *E. coli* in the presence of H_2O_2 [19]. Novel cerium-silver nanozymes completely kill MRSA and *S. aureus* along with the prolong the action time [150].

5.9. Antitumor applications

The antitumor effect can be reinforced based on the multi-species enzymatic activity of CeO_2 NZs. The amphiphilic peptide conjugated CeO_2 NZs combined with PDT treatment result in a significant increase in ROS levels in tumor cells to achieve the significant tumor growth inhibition [151]. Linear Cu-doped CeO_2 NZs combined with Doxorubicin treatment exhibit a threefold reduction in tumor volume compared to that of the mice treated with Doxorubicin alone [152]. Based on the OXD- and POD-mimetic cascade catalytic activities of CeO_2 NZs, O_2 can be directly catalyzed to $^{\bullet}OH$. However, the tumor microenvironment is hypoxic. CeO_2 NZs can also exert CAT-mimetic activities to decompose H_2O_2 into produce O_2 and alleviate tumor hypoxia [102].

5.10. Limitations and prospective analysis of the clinical translation of CeO_2 NZs

The potential clinical perspectives of the above applied studies have been demonstrated in Table 3. CeO_2 NZs have shown great potential in multi-stage intervention of diseases, ranging from antioxidation, anti-inflammation to protecting damaged tissues. Through surface modification and cell membrane biomimetic modification, CeO_2 NZs have achieved precise delivery and multi-target therapeutic effect. In addition, CeO_2 NZs have the function of combining diagnosis and treatment. It can monitor the distribution of CeO_2 NZs in the body in real time, evaluate its therapeutic effect, and provide new strategies for the early diagnosis and intervention of diseases. Despite the biomedical potential of CeO_2 NZs, less progress has been achieved in translating it into clinical practice due to safety and technical aspects. Safety is always an important criterion for application. Most of the articles focus on the therapeutic effect of CeO_2 NZs, and the safety only included cytotoxicity assays, hemolytic assays, and hematoxylin-eosin staining, *etc*. Here is a four-point summary of the safety challenges faced during the clinical translation of CeO_2 NZs, which are more important to consider while designing high-performance CeO_2 NZs nanocomplexes.

The first is long-term toxicity. It has been shown that the density of hepatocyte apoptosis is maximized on day 30 after the time of CeO_2 NZs administration [153]. Under prolonged exposure, CeO_2 NZs enable to penetrate the alveolar space and induce a sustained inflammatory response [154]. Most studies focus on about 14 days after administration, which is insufficient to observe the long-term toxicity of CeO_2 NZs. The second is high-dose toxicity. Long-term exposure to higher CeO_2 NZs doses (>100 mg/kg) cause enteritis and changes in intestinal flora compositions [155]. Most studies only set a single dose in animal studies and lack an examination of dose toxicity. This failure to establish a safe dosage range hinders clinical translation. In the future, different dose groups should be established *in vivo* biosafety analyses, especially higher dose groups, to determine the dose threshold toxicity occurs. The third is the effect of different administration routes. It has been shown that intravenously and intraperitoneally administered CeO_2 NZs show maximum deposition in spleen followed by liver, lungs and kidneys. Oral administration does not lead to significant accumulation in any organ except lungs [156]. Exploring appropriate routes of administration that bring out less accumulation in non-target tissues and lower toxicity in specific diseases can accelerate the clinical translation of CeO_2 NZs. The fourth is the stabilization in physiological media involving the appropriate interactions with the body. Modification strategies to improve stability are also mentioned in the previous section.

6. Summary and outlook

In this review, the catalytic properties of CeO_2 NZs and influencing factors are described. The green preparation methods are simple, environmentally friendly, and conducive to the stabilization of CeO_2 NZs, including plant, microbial, and food-mediated.

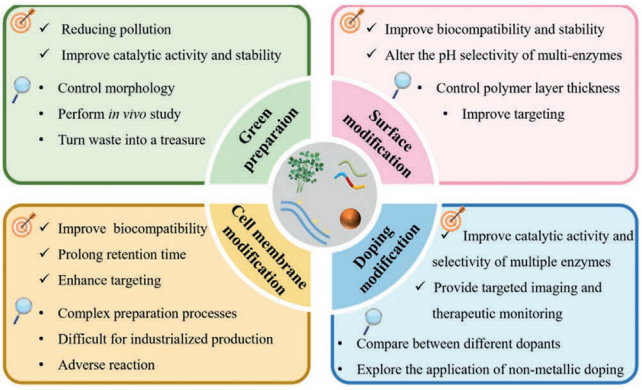


Fig. 7. The important role of CeO_2 NZs improvement methods in the biomedical field and the challenges.

Surface modification, cell membrane biomimetic modification, and metal doping to reinforce the stability, biocompatibility, targeting and to improve the mimetic enzyme activity and selectivity of CeO_2 NZs are discussed. To date, CeO_2 NZs, a biomedical tool with great potential, have presented promising research perspectives in the fields of disease therapy.

Improvements in the preparation and properties of CeO_2 NZs advance its research in the biomedical field. Fig. 7 summarizes the important role of CeO_2 NZs improvement methods in the biomedical field and the challenges. In addition to limited morphological diversity, the lack of *in vivo* studies is also a limitation of the green preparation technique. Consequently, it is extremely necessary to further explore the stability, biocompatibility and activity of green synthesized CeO_2 NZs. In surface modification, it is essential for the screening of appropriate coating thickness to modulate the properties of CeO_2 NZs. Thinner-coated CeO_2 NZs can be prepared by *in situ* procedures and thicker coated CeO_2 NZs by a stepwise procedure [39]. In the bionic cell membrane modification methods, it is more difficult to industrialized production attributed to the complicated preparation process [77]. Future work should simplify cell membrane extraction or explore artificial membranes as alternatives. Moreover, it is necessary to investigate whether the proteins on certain cell membranes cause adverse effects on the human body. For doping modification, it still lacks the comparison between different metal dopants. In subsequent studies, computational simulations can be performed by methods such as density functional theory to reveal how different dopants affect the catalytic process of CeO_2 NZs. Comparison of free radical scavenging and *in vitro* antimicrobial experiments also should be carried out to obtain metal-doped CeO_2 NZs with higher activity.

To identify the core competencies and potential risks of CeO_2 NZs in the biomedical field, it is vitally essential to conduct a comprehensive analysis of the strengths, weaknesses, opportunities, and threats (SWOT) of CeO_2 NZs as shown in Fig. S1 (Supporting information). Currently, CeO_2 NZs still lack a standardized clinical efficacy assessment protocol, and the absorption, distribution, metabolism, excretion process in humans is unclear. The liver and spleen are currently considered to be the main organs where CeO_2 NZs accumulates and distributes [113]. Therefore, safety studies should be performed for the liver and spleen. Monitoring of cerium concentrations in tissues at different days after administration or the use of cerium tracking techniques are possible methods to assess the distribution of CeO_2 NZs *in vivo*. Additionally, the metabolism and excretion of CeO_2 NZs can be informed by long-term monitoring of its timely removal. Large-scale production of CeO_2 NZs products has not been broken through yet. Consequently, process amplification, equipment selection, process design and other aspects are very important. Meanwhile, it is necessary to realize green production of CeO_2 NZs as much as possible.

Declaration of competing interest

The authors declare that they have no known competing financial interests or personal relationships that could have appeared to influence the work reported in this paper.

CRediT authorship contribution statement

Zhixuan Li: Writing – review & editing, Writing – original draft, Conceptualization. **Xinying Wang:** Writing – review & editing. **Han Wu:** Writing – review & editing. **Qingxiang Guan:** Resources, Project administration, Funding acquisition.

Acknowledgment

This work was supported by Concept Verification Fund of Jilin University (No. 2024GN034).

Supplementary materials

Supplementary material associated with this article can be found, in the online version, at doi:10.1016/j.cclet.2025.111671.

References

[1] R.F. Zhang, X.Y. Yan, K.L. Fan, Acc. Mater. Res. 2 (2021) 534–547.
[2] Y.J. Dai, Y.M. Ding, L.N. Li, Chin. Chem. Lett. 32 (2021) 2715–2728.
[3] B.A. Baldo, Biodrugs 29 (2015) 31–55.
[4] F. Manea, F.B. Houillon, L. Pasquato, et al., Angew. Chem., Int. Ed. 43 (2004) 6165–6169.
[5] L.Z. Gao, J. Zhuang, L. Nie, et al., Nat. Nanotechnol. 2 (2007) 577–583.
[6] R.F. Zhang, B. Jiang, K.L. Fan, et al., Nat. Rev. Bioeng. 2 (2024) 849–868.
[7] Y.Y. Huang, J.S. Ren, X.G. Qu, Chem. Rev. 119 (2019) 4357–4412.
[8] M. Liu, Z.H. Li, Y.X. Li, et al., Chin. Chem. Lett. 30 (2019) 1009–1012.
[9] Y.D. Bai, Y.M. Li, Y.M. Li, et al., ACS Omega 9 (2024) 8601–8614.
[10] G.G. Zhou, W.T. Geng, L. Sun, et al., Materials 12 (2019) 4041.
[11] M.A. Saifi, S. Seal, C. Godugu, J. Control. Release 338 (2021) 164–189.
[12] R.X. Wang, Y.Y. Du, Y. Fu, et al., ACS Sens. 8 (2023) 4442–4467.
[13] Y.G. Kim, Y. Lee, N. Lee, et al., Adv. Mater. 36 (2024) 2210819.
[14] F. Charbgoo, M. Bin Ahmad, M. Darroudi, Int. J. Nanomed. 12 (2017) 1401–1413.
[15] M. Khan, Z.U.R. Mashwani, M. Ikram, et al., Nanomaterials 12 (2022) 2117.
[16] Y. He, E.J. Peng, X.Z. Ba, et al., Small 21 (2024) 2405417.
[17] B.W. Liu, J.W. Liu, Nano Res. 10 (2017) 1125–1148.
[18] J.G. Shan, L. Du, X.G. Wang, et al., Adv. Sci. 11 (2024) 2304441.
[19] P. Jiang, L.D. Zhang, X.L. Liu, et al., Nat. Commun. 15 (2024) 1010.
[20] N. Sisubalan, C. Karthikeyan, V.S. Kumar, et al., RSC Adv. 11 (2021) 30623–30634.
[21] C. Xu, X.G. Qu, NPG Asia Mater. 6 (2014) e90.
[22] J. Zhang, Z.H. Wang, X.E. Lin, et al., Angew. Chem. Int. Ed. 64 (2024) e202416686.
[23] P.H. Lin, M.D. Cao, F. Xia, et al., Adv. Sci. 8 (2021) 2004115.
[24] M.D. Jin, Z. Liang, Y.K. Huang, et al., J. Am. Chem. Soc. 146 (2024) 34092–34106.
[25] T. Pirmohamed, J.M. Dowding, S. Singh, et al., Chem. Commun. 46 (2010) 2736–2738.
[26] C. Korsvik, S. Patil, S. Seal, et al., Chem. Commun. (2007) 1056–1058.
[27] S. Yadav, S. Chamoli, P. Kumar, et al., Int. J. Biol. Macromol. 246 (2023) 125673.
[28] K.O. Abdulwahab, M.M. Khan, J.R. Jennings, ACS Omega 8 (2023) 30802–30823.
[29] E. Shoko, M.F. Smith, R.H. McKenzie, J. Phys. Condens. Matter 22 (2010) 223201.
[30] S. Deshpande, S. Patil, S. Kuchibhatla, et al., Appl. Phys. Lett. 87 (2005) 133113.
[31] H.Y. Li, X.Q. Wang, H. Yi, et al., Catal. Today 426 (2024) 114398.
[32] W.T. Yang, X. Wang, S.Y. Song, et al., Chem 5 (2019) 1743–1774.
[33] D.H. Youn, N.M. Tran, T.N. Nguyen, et al., J. Am. Chem. Soc. 106 (2023) 7218–7229.
[34] J. Li, Z.Y. Zhang, Z.M. Tian, et al., J. Mater. Chem. A 2 (2014) 16459–16466.
[35] Z.M. Tian, J. Li, Z.Y. Zhang, et al., Biomaterials 59 (2015) 116–124.
[36] C. Liu, L. Gui, J.J. Zheng, et al., J. Am. Chem. Soc. 145 (2023) 19086–19097.
[37] Q. Weng, H. Sun, C. Fang, et al., Nat. Commun. 12 (2021) 1436.
[38] X.L. Liu, J.J. Wu, Q.Y. Liu, et al., J. Mater. Chem. B 9 (2021) 7238–7245.
[39] A. Asati, S. Santra, C. Kaittanis, et al., Angew. Chem. Int. Ed. 121 (2009) 2344–2348.
[40] X. Jiao, H.J. Song, H.H. Zhao, et al., Anal. Methods 4 (2012) 3261–3267.

[41] S. Pandey, S. Kumari, L.M. Aeshala, et al., J. Biomater. Appl. 38 (2024) 866–874.
[42] S.Y. Gao, D. Yu, S.R. Zhou, et al., J. Mater. Chem. A 11 (2023) 19210–19243.
[43] H.Y. Zhou, X.L. Jiang, Q. Han, et al., Chem. Eng. J. 515 (2025) 163665.
[44] A. Selmani, D. Kovacevic, K. Bohinc, Adv. Colloid Interface Sci. 303 (2022) 102640.
[45] T.P. Yadav, O.N. Srivastava, Ceram. Int. 38 (2012) 5783–5789.
[46] B.S. Wee, S.A.B. Halim, T.F. Choo, J. Cluster Sci. 35 (2024) 2061–2068.
[47] D.J. Kang, X.L. Yu, M.F. Ge, Chem. Eng. J. 330 (2017) 36–43.
[48] F.J. Chen, P.L. Ho, R. Ran, et al., J. Alloys Compd. 714 (2017) 560–566.
[49] A. Balamurugan, M. Sudha, S. Surendhiran, et al., Mater. Today: Proc. 26 (2020) 3588–3594.
[50] J.Y. Bai, Z.D. Xu, Y.F. Zheng, et al., Mater. Lett. 60 (2006) 1287–1290.
[51] A. Chitsaz, M. Jalilpour, M. Fathalilou, Int. J. Mater. Res. 104 (2013) 511–514.
[52] M. Nadeem, R. Khan, K. Afridi, et al., Int. J. Nanomed. 15 (2020) 5951–5961.
[53] D. Dutta, R. Mukherjee, M. Patra, et al., Colloids Surf. B 147 (2016) 45–53.
[54] D. Ayodhya, A. Ambala, G. Balraj, et al., Results Chem. 4 (2022) 100441.
[55] A. Arumugam, C. Karthikeyan, A.S.H. Hameed, et al., Mater. Sci. Eng. C 49 (2015) 408–415.
[56] S. Awan, A. Sajjad, Z. Ali, et al., Emergent Mater. 7 (2024) 1129–1138.
[57] M. Khan, N.I.R. Sohail, et al., Sci. Rep. 13 (2023) 4514.
[58] J. Mim, M.S. Sultana, P.K. Dhar, et al., RSC Adv. 14 (2024) 25409–25424.
[59] T.L. Pushparaj, E.F.I. Raj, E.F.I. Rani, et al., Biomass Convers. Biorefin. 15 (2023) 1327–1341.
[60] F.J. Trindade, S. Damasceno, L. Otubo, et al., ACS Appl. Nano Mater. 5 (2022) 8859–8867.
[61] N. Pandiyan, B. Murugesan, J. Sonamuthu, et al., Ceram. Int. 45 (2019) 12138–12148.
[62] N. Pandiyan, B. Murugesan, J. Sonamuthu, et al., J. Photochem. Photobiol. B 178 (2018) 481–488.
[63] J. Malleshappa, H. Nagabhushana, D. Kavyashree, et al., Spectrochim. Acta Part A 145 (2015) 63–75.
[64] J.C. Qian, F. Chen, X.B. Zhao, et al., J. Nanopart. Res. 13 (2011) 7149–7158.
[65] S.A. Khan, A. Ahmad, Mater. Res. Bull. 48 (2013) 4134–4138.
[66] K.S. Venkatesh, K. Gopinath, N.S. Palani, et al., RSC Adv. 6 (2016) 42720–42729.
[67] K. Gopinath, V. Karthika, C. Sundaravadivelan, et al., J. Nanostruct. Chem. 5 (2015) 295–303.
[68] M. Darroudi, S.J. Hoseini, R.K. Oskuee, et al., Ceram. Int. 40 (2014) 7425–7430.
[69] H. Kargar, H. Ghazavi, M. Darroudi, Ceram. Int. 41 (2015) 4123–4128.
[70] S.N. Patil, J.S. Paradeshi, P.B. Chaudhari, et al., Appl. Biochem. Biotechnol. 180 (2016) 638–654.
[71] H. Siddiqui, S. Kumar, P. Naidu, et al., Chemosphere 352 (2024) 141418.
[72] B. Chanteau, J. Fresnais, J.F. Berret, Langmuir 25 (2009) 9064–9070.
[73] S. Das, P.R. McDonagh, T.S. Sakthivel, et al., Environ. Toxicol. 32 (2017) 904–917.
[74] W.C. Peng, W.B. Tai, B.W. Li, et al., Nat. Mater. 24 (2024) 637–648.
[75] N. Yadav, 3 Biotech 12 (2022) 121.
[76] A.A. Yetisgin, S. Cetinel, M. Zuvin, et al., Molecules 25 (2020) 2193.
[77] Y. Liu, J.S. Luo, X.J. Chen, et al., Nano-Micro Lett. 11 (2019) 100.
[78] J. Liu, Y. Zhu, Y. Fan, et al., J. Colloid Interface Sci. 654 (2024) 1054–1062.
[79] S.M. Wei, Y.Q. Yang, J.J. Li, et al., Chin. Chem. Lett. 35 (2024) 109114.
[80] S.Y. Qian, H.Y. Zhang, X.X. Sun, et al., Sens. Actuators B: Chem. 383 (2023) 133609.
[81] J. Chen, Y. Liu, Z.R. Long, et al., Chin. Chem. Lett. 35 (2024) 109463.
[82] G. Bübül, A. Hayat, S. Andreescu, Adv. Healthc. Mater. 5 (2016) 822–828.
[83] H. Li, Z.Y. Yang, C. Liu, et al., Free Radical Biol. Med. 87 (2015) 26–35.
[84] X.H. Ju, M.H. Kalbacova, B. Smd, et al., J. Mater. Chem. B 9 (2021) 7386–7400.
[85] M.Y. Zhu, Y.F. Wen, S.G. Song, et al., Nanoscale 12 (2020) 19104–19111.
[86] E. Alpaslan, B.M. Geilich, H. Yazici, et al., Sci. Rep. 7 (2017) 45859.
[87] E. Alpaslan, H. Yazici, N.H. Golshan, et al., ACS Biomater. Sci. Eng. 1 (2015) 1096–1103.
[88] Y. Cao, K. Cheng, M. Yang, et al., J. Nanobiotechnol. 21 (2023) 21.
[89] M.A. Davoodbasha, K. Saravanakumar, A.M. Abdulkader, et al., ACS Appl. Bio Mater. 2 (2019) 1792–1801.
[90] G. Kermani, E. Karimi, M.H. Tabrizi, J. Inorg. Organomet. Polym. Mater. 32 (2022) 2591–2599.
[91] J.M. Perez, A. Asati, S. Nath, et al., Small 4 (2008) 552–556.
[92] R.P. Senthilkumar, V. Bhuvaneshwari, R. Ranjithkumar, et al., Int. J. Biol. Macromol. 104 (2017) 1746–1752.
[93] S. Wang, J.W. Zhang, W. Li, et al., Carbohydr. Polym. 296 (2022) 119940.
[94] S.S. Lee, W.S. Song, M.J. Cho, et al., ACS Nano 7 (2013) 9693–9703.
[95] H. Xu, K.Q. Wang, Y.H. Deng, et al., Biomaterials 31 (2010) 4757–4763.
[96] G.F. Chen, L. Cui, P. Luo, et al., ACS Appl. Mater. Interfaces 16 (2024) 34705–34719.
[97] F. Cheng, S.Q. Wang, H. Zheng, et al., Colloids Surf. B 205 (2021) 111878.
[98] H. Dong, J. Li, X.Y. Huang, et al., Int. J. Biol. Macromol. 251 (2023) 126393.
[99] X.X. Fu, X.J. Yu, J.H. Jiang, et al., Nat. Commun. 13 (2022) 6528.
[100] X.Y. Hu, X.H. Zhang, G.X. Zhang, et al., Nanoscale 16 (2024) 22312–22325.
[101] Y. Li, D.F. Liu, T. Chen, et al., Adv. Funct. Mater. 34 (2024) 2403183.
[102] Z. Li, J.X. Bian, Z.C. Xu, et al., ACS Appl. Mater. Interfaces 15 (2023) 56869–56880.
[103] X.F. Song, Z.Y. Zheng, S.X. Ouyang, et al., ACS Appl. Mater. Interfaces 15 (2023) 33239–33249.
[104] Y.F. Li, X.L. Xu, H.J. Wang, et al., Arterioscler., Thromb., Vasc. Biol. 44 (2024) e82–e98.
[105] B. Beck-Schimmer, C. Madjdpour, S. Kneller, et al., Eur. Respir. J. 19 (2002) 1142–1150.
[106] C.J. Shuai, K.D. Wang, S.P. Peng, et al., Surf. Interfaces 45 (2024) 103846.
[107] K. Saravanakumar, A. Sathiyaseelan, V.V. Priya, et al., J. Drug Deliv. Sci. Technol. 72 (2022) 103367.
[108] S.N. Naidi, F. Khan, A.L. Tan, et al., New J. Chem. 45 (2021) 7816–7829.
[109] S.Z. Zhao, D.J. Kang, Y.P. Liu, et al., ACS Catal. 10 (2020) 11739–11750.
[110] P.T. Nguyen, J. Lee, A. Cho, et al., Adv. Funct. Mater. 32 (2022) 2112428.
[111] W.J. Guo, M. Zhang, Z.P. Lou, et al., ChemCatChem 11 (2019) 737–743.
[112] Z.M. Alaizeri, H.A. Alhadlaq, S. Aldawood, et al., J. Radiat. Res. Appl. Sci. 17 (2024) 100889.
[113] E. Casals, M.L. Zeng, M. Parra-Robert, et al., Small 16 (2020) 1907322.
[114] X. Chen, L.L. Wang, J.T. Zhang, et al., Adv. Healthc. Mater. 13 (2024) 2401507.
[115] C. Feng, Z.L. Xiong, X.T. Sun, et al., Biomaterials 299 (2023) 122164.
[116] Y. Hu, H. Guo, S. Cheng, et al., Int. J. Nanomed. 18 (2023) 6797–6812.
[117] Q. Huang, J. Liao, J.J. Li, et al., Chin. Chem. Lett. 36 (2025) 109914.
[118] Y.B. Huang, J.Q. Xu, G. Sun, et al., Biomaterials 314 (2024) 122822.
[119] X. Li, Z.H. Han, T.Y. Wang, et al., Biomaterials 291 (2022) 121904.
[120] J. Liao, Y. Li, L. Fan, et al., ACS Nano 18 (2024) 5510–5529.
[121] H.B. Liu, M.S. Ji, Y.T. Bi, et al., J. Control. Release 361 (2023) 493–509.
[122] A. Patel, J. Kosanovich, S. Sansare, et al., Bioact. Mater. 24 (2023) 124–135.
[123] C.C. Wang, X.L. Song, P. Li, et al., ACS Appl. Mater. Interfaces 16 (2024) 27127–27138.
[124] T.T. Wang, W.F. Guo, X.X. Lv, et al., Adv. Funct. Mater. 34 (2024) 2404774.
[125] P. Wei, Y.F. Wang, H.Y. Feng, et al., Small 20 (2024) 2404463.
[126] Y.H. Zhang, W.L. Liu, G. Wei, et al., ACS Nano 18 (2024) 9019–9030.
[127] C.Y. Zhao, L. Huang, J. Tang, et al., Int. J. Biol. Macromol. 278 (2024) 134597.
[128] S.H. Zhao, J.H. Ling, N. Wang, et al., Chem. Eng. J. 497 (2024) 154517.
[129] C.C. Xie, J. Liao, N. Zhang, et al., Chin. Chem. Lett. 35 (2024) 109149.
[130] H.H. Zeng, Y.J. Qi, Z.Y. Zhang, et al., Chin. Chem. Lett. 32 (2021) 1857–1868.
[131] J. Yang, G. Qin, Z.Q. Liu, et al., Nano Lett. 24 (2024) 9906–9915.
[132] K.Z. Ge, Y.F. Mu, M.Y. Liu, et al., ACS Appl. Mater. Interfaces 14 (2022) 3662–3674.
[133] L. Chen, Y. Du, K. Zhang, et al., ACS Nano 12 (2018) 1321–1338.
[134] R.Y. Yan, X. Zhang, W.L. Xu, et al., Aging Dis. 16 (2025) 250–268.
[135] B. Tirosh, N. Khatib, Y. Barenholz, et al., Mol. Pharm. 6 (2009) 1083–1091.
[136] M.Y. Li, J. Liu, L. Shi, et al., Bioact. Mater. 25 (2023) 95–106.
[137] D.K. Min, Y.E. Kim, M.K. Kim, et al., ACS Nano 17 (2023) 24404–24416.
[138] S. Zhao, Y.X. Li, Q.Y. Liu, et al., Adv. Funct. Mater. 30 (2020) 2004692.
[139] R.H. Deng, R.F. Zhao, Z.N. Zhang, et al., Sci. Transl. Med. 16 (2024) eadh9751.
[140] S. Koo, H.S. Sohn, T.H. Kim, et al., Nat. Nanotechnol. 18 (2023) 1502–1514.
[141] H. Fu, Y.D. Guo, W.M. Fang, et al., Adv. Sci. 11 (2024) 2307094.
[142] L.L. Cui, J.H. Liang, H. Liu, et al., Tissue Eng. Part B: Rev. 26 (2020) 203–216.
[143] M. Berthet, Y. Gauthier, C. Lacroix, et al., Trends Biotechnol. 35 (2017) 770–784.
[144] H. Chang, P.F. Tian, L.Z. Hao, et al., Chem. Eng. J. 481 (2024) 148768.
[145] Y.J. Xue, F. Yang, Y.J. He, et al., Adv. Healthc. Mater. 14 (2025) 2402236.
[146] A.I. Dogaru, O.C. Oprea, G.O. Isopencu, et al., Polymers 17 (2025) 1225.
[147] Y. Feng, D. Zhang, X.Y. Chen, et al., Adv. Funct. Mater. 34 (2023) 2307157.
[148] M.Z. Zhang, C. Zhang, X.Y. Zhai, et al., Sci. China Mater. 62 (2019) 1727–1739.
[149] H. Nosrati, M. Heydari, M. Khodaei, Mater. Today Bio 23 (2023) 100823.
[150] A.S. Pugazhendhi, C.J. Neal, K.M. Ta, et al., Biomaterials 307 (2024) 122527.
[151] X. Luo, Q.S. Jiao, S.C. Pei, et al., Adv. Healthc. Mater. 13 (2024) 2401787.
[152] Z.X. Gu, D. Zhong, X.Y. Hou, et al., Adv. Sci. 11 (2024) 2307154.
[153] M.T. Tseng, X.Q. Lu, X.X. Duan, et al., Toxicol. Appl. Pharmacol. 260 (2012) 173–182.
[154] D. Schwotzer, H. Ernst, D. Schaudien, et al., Part. Fibre Toxicol. 14 (2017) 23.
[155] Q.R. Ye, D.T. Jia, J. Ji, et al., PLoS One 19 (2024) e0304806.
[156] S.M. Hirst, A. Karakoti, S. Singh, et al., Environ. Toxicol. 28 (2013) 107–118.